Title
Metabolic Regulation of Cell Identity and Therapy Response in Prostate Cancer

Author
Atmakuri, Aishwarya

Publication Date
2022-06-03

Undergraduate

Aishwarya Atmakuri

Metabolic regulation of cell identity and therapy response in prostate cancer

1. ABSTRACT

Prostate cancer growth is driven by androgen signaling using the androgen receptor (AR). Androgen deprivation therapy (ADT) is the gold standard for prostate cancer, but the majority of ADT-treated patients develop resistance, which often involves the loss of luminal lineage identity and AR-independent growth. Previous work has shown that modulating metabolism can regulate cell fate in many tissues. Therefore, it is important to understand the mechanisms behind how altered metabolism affects lineage identity and response to AR blockade, a common form of treatment for prostate cancer involving blocking AR signaling. Inhibition of mitochondrial pyruvate carrier 1, an essential metabolic enzyme, with small molecule UK5099 in mouse basal-derived nonmalignant organoids blocked luminal differentiation and UK5099-treated organoids retained a basal phenotype. AR expression decreased substantially in vehicle-treated organoids, but had a more modest decrease in UK5099-treated organoids in castrated conditions. Expression of Tmprss2, an AR target gene, slightly decreased in vehicle-treated organoids, yet slightly increased with UK5099 treatment in castrated conditions. The organoid size assay was a useful tool in determining how modulating metabolism affected the impact of castration on organoid diameter in 3D *ex vivo* organoid culture. It shows that the number of days post-castration onset could affect the relative size of different treatment groups, but 6 days after castration vehicle-treated organoids were smaller in castrated conditions than control conditions. Castrated UK5099-treated organoids, however, appeared slightly larger than the UK5099 control. An investigation

into differentiation and metabolic pathways affected by UK5099-treatment revealed differential expression of phosphorylated p-65 (NFkB), changes in β-catenin nuclear translocation, and increased citrate synthase, OGDH, and MDH2 in the nucleus. This shows that UK5099 affects both differentiation and metabolism. Collectively, these results show that altering metabolism affects lineage identity and response to AR blockade. Modulation of metabolism appears to be a potential method of improving clinical outcomes for advanced prostate cancer.

2. INTRODUCTION

The prostate is an important component of the male reproductive system. It secretes fluid that nourishes and transports sperm. Prostate cancer is the result of malignant, uncontrollable proliferation of a cell in the prostate. 1 in 8 men will be diagnosed with prostate cancer in his lifetime, and over 34,000 men in the United States will die from prostate cancer in 2021[1]. Prostate cancer growth is driven by the androgen receptor (AR), which is also a transcription factor[2,3]. High serum levels of prostate specific antigen (PSA) has been used to screen for prostate cancer and indicate that increased AR activity is associated with prostate cancer[3,4]. AR is a transcription factor that becomes activated and translocates to the nucleus after binding to dihydrotestosterone (DHT), the more potent intracellular reduced form of testosterone[2,3]. AR is important for prostate cancer progression and migration[5,6]. Androgen deprivation therapy (ADT) targets AR signaling and is the standard treatment for prostate cancer. Such therapy can select for AR-independent phenotypes that lead to therapy resistance with AR-independent mechanisms of growth[7]. The majority of ADT-treated patients develop castration resistant prostate cancer (CRPC) after 2-3 years[8]. CRPC may be due to ligand-independent AR activation, increased levels of AR expression, mutations that make AR insensitive to anti-androgen treatment, or alterations in androgen metabolism[2,3,9].

Recent research has also identified epigenetic events as a potential mechanism leading to CRPC[10,11]. CRPC is treated with Enzalutamide, an androgen receptor pathway inhibitor[12,13]. While initially effective, most cancers develop resistance (Figure 1). Gene set enrichment analysis of Enzalutamide-resistant tumors shows that nonresponders had low AR transcriptional activity and a stem-like program, indicating AR-independent growth and proliferation[14]. One mechanism behind this is a change in lineage identity primarily characterized by a loss of luminal features and the development of basal and neuroendocrine features[15,16]. Basal and luminal cells are both epithelial cells in the prostate. Basal cells sit on the basement membrane and contribute to the structural integrity of the prostate, while luminal cells produce secretory proteins important for prostate function[17,18]. Luminal cells are highly AR-dependent for growth[19]. Studying the mechanisms that regulate lineage identity can lead to new approaches to reduce therapy resistance and improve therapeutic outcomes.

Treatment-resistant prostate cancers are increasingly associated with a loss of luminal phenotype[15]. The Goldstein Laboratory has previously shown that altering metabolism through mitochondrial pyruvate carrier (MPC) inhibition (through UK5099 treatment) blocks luminal differentiation and promotes a more basal phenotype. Other studies have also found that metabolism can regulate cell fate in many tissues[20–22]. In mammary epithelial cells, there have been enriched glycolytic metabolic networks in basal cells and oxidative phosphorylation in the luminal lineage, similar to what has been previously shown by the effects of MPC inhibition[22]. In epidermal stem cells, endogenous serine synthesis facilitates histone demethylation, which later regulates differentiation. Altering the metabolic environment can also impair tumor formation and response to oncogenic stress[23]. In the intestinal crypt, mitochondrial signaling has been shown to drive cellular differentiation in crypt base columnar cells and Paneth cells[20]. MPC signaling

regulates cell proliferation through promoting pyruvate metabolism in the mitochondria in the intesting[24]. In skeletal stem cells, glutamine metabolism can modulate osteoblast and adipocyte specification[21]. The interplay between metabolism and lineage identity in the prostate must be further elucidated to understand its role in therapy response.

In this project, I will evaluate how MPC inhibition alters sensitivity to AR blockade to understand how regulation of lineage identity through metabolism can affect response to therapy. I will also investigate metabolic and differentiation pathways that are involved in UK5099 action. Preliminary data has shown that castrated conditions (absence of dihydrotestosterone) cause a decrease in luminal marker expression. Furthermore, UK5099-treated organoids exhibit reduced sensitivity to castration relative to vehicle-treated organoids.

3. METHODS

Cell Culture

Primary mouse-derived prostate cells were collected from wild type mice. Prostate was dissected and then processed into single cells using dissociation media (RPMI base media with 10% FBS, 1% penicillin and streptomycin, and DNase and ROCK inhibitor (RI) added. Cells were centrifuged, washed in PBS, and incubated in trypsin. Cells were syringed, filtered, centrifuged, and resuspended in dissociation media. Cell sorting antibodies and DAPI were used to prepare cells for fluorescence-activated cell sorting. Basal cells were isolated using EpCAM+ and CD49f^{high} cells.

3D organoid culture has been shown to be an representative model of the prostate and include both basal and luminal cells[25]. Primary mouse-derived basal cells were plated into Matrigel in organoid culture at 2500 cells/well on 24-well tissue culture plates with poly-HEMA coating

with 350 µL to 1000 µL of fresh media based on organoid size. Media was changed every 48 hours. Control mouse organoid media consisted 34.5 mL advanced DMEM F12, 5 mL R-spondin conditioned media, 1 mL B27, 500 µL Glutamax, 125 µL NAC, 50 µL Normocin, 50 µL Noggin, 50 µL DHT, 5 µL EGF, and 5 µL A-8301. Castrated media was the same as control mouse organoid media, except with no DHT. Both UK5099 and Enzalutamide were added to media at 10 µM concentration with vehicle control DMSO. Vehicle and UK5099 pretreatment started when cells were plated, and Enzalutamide and castration treatment started 96 hours after plating.

Organoids were harvested using dispase containing media (1 mg dispase per mL advanced DMEM F12 + RI 1:1000). Media was removed, Matrigel was blasted with the harvesting media, and collected cells incubated in harvesting media for 30 minutes to 1 hour. Cells were centrifuged, resuspended in PBS, and centrifuged and then PBS was removed. Cells pellets were flash frozen in dry ice and methanol and stored in -80˚C.

Western Blot

Cell pellets were resuspended in 40 – 300 µL of RIPA buffer containing protease inhibitors and phosphatase inhibitors depending on pellet size. Pellets were sonicated and then placed on ice for 30 minutes. Pellets were stored at -20˚C.

A BCA assay was used to find the concentration of protein in each sample. The assay generated a standard curve based on absorbance, which was used to calculate protein concentration of each sample to ensure even loading.

Each lane was loaded with 10 µg protein, loading buffer, reducing agent, and water to ensure even volumes. Master mixes for each sample were boiled at 70˚C for 10 minutes and then cooled on ice for 5 minutes. Samples were loaded onto NuPAGE™ 4 to 12% Bis-Tris gels and ran with running buffer (40 mL 20x MOPS NuPAGE SDS running buffer and 760 mL DI H_2O, inner

chamber had added 500 µL NuPAGE antioxidant). Blue2 Plus protein ladder was used to identify protein location. Gels ran at 200 V for 50 minutes.

Gels were transferred onto a PVDF membrane in a Wattmann paper sandwich after full submersion in transfer buffer (15 mL 20x NuPAGE transfer buffer, 0.3 mL NuPAGE antioxidant, 30 mL methanol, 255 mL DI H_2O. Wet transfer ran at 30 V for 1 hour. Membrane was removed and allowed to dry after transfer.

SYPRO Ruby Stain was used to ensure even loading and no air bubbles in regions of interest. The dried membrane was floated in fixation solution (5 mL methanol, 3.5 mL acetic acid, 41.5 mL water) for 15 minutes. Membrane was then washed with water 4 times for 5 minutes and then floated face down in SYPRO Ruby for 15 minutes. Membrane was again washed 4 times for 1 minute and air dried.

Membrane was then trimmed to allow for multiple proteins to be probed for. Methanol-activated membrane was blocked in 5% PBST milk for 1 hour and then primary antibody was added overnight. Membrane was washed in PBST 3 times for 5 minutes. Membrane was then placed in secondary antibody in 5% PBST milk for 1 hour. Membrane was washed with PBST 3 times for 5 minutes for fluorescent detection and 6 times for 5 minutes for chemiluminescent detection.

Fluorescent detection used Alexa Fluor® 647 conjugated antibodies and were using the iBright 1500 imaging system. Chemiluminescent antibodies were read using horseradish peroxidase substrates.

Organoid Size Quantification

Organoid quantification used 25 representative images of organoids in each sample taken on a phase contrast microscope. The diameter of each organoid image was assessed and averaged

to quantify average organoid size. Organoids were cultured in vehicle or 10 μM UK5099 media for 4 days pre-treatment followed by 6 days of treatment with control, castrated (-DHT), or 10 μM Enzalutamide.

Subcellular Fractionation

Used ThermoFisher Scientific Subcellular Protein Fractionation Kit for Cultured Cells (number 78840). Kit enables stepwise separation of cytoplasmic, membrane, nuclear soluble, chromatin-bound, and cytoskeletal protein extracts from whole cell lysate. First, cells were incubated in cytoplasm extraction buffer (CEB) for 10 minutes, centrifuged at 500g for 5 minutes, and supernatant containing cytoplasmic extract was transferred to a separate tube. Cell pellets were washed and centrifuged with the same amount of PBST. Cells were then incubated in membrane extraction buffer (MEB) with protease inhibitors, vortexed, incubated for 10 minutes, centrifuged at 3000g for 5 minutes, and supernatant containing membrane extract was transferred to a separate tube. Cell pellets were washed and centrifuged with the same amount of PBST. Cells were then incubated in nuclear extraction buffer (NEB) with protease inhibitors, vortexed, incubated for 30 minutes, centrifuged at 500g for 5 minutes, and supernatant containing soluble nuclear extract was transferred to a separate tube. Cell pellets were washed and centrifuged with the same amount of PBST. Cells were then incubated in nuclear extraction buffer (NEB) with protease inhibitors, $CaCl_2$, and micrococcal nuclease, vortexed, incubated for 15 minutes, centrifuged at 500g for 5 minutes, and supernatant containing nuclear chromatin-bound extract was transferred to a separate tube.

4. Results

Blocking mitochondrial pyruvate uptake blocks luminal differentiation

The Goldstein Laboratory has previously shown that mitochondrial pyruvate carrier (MPC) inhibition using UK5099 (K_i = 49μM) blocks luminal differentiation and promotes a more basal phenotype. Given that prostate cancer growth is driven by AR and that existing therapies target the AR signaling axis, I first investigated the effect of UK5099 on AR expression and validated the change in luminal identity in basal-derived organoids (Figure 2a).

AR expression did not change between vehicle and UK5099 treatment. The luminal marker K8, however, did decrease in UK5099-treated organoids. Typically, vehicle-treated basal-derived organoids differentiate from basal to luminal over the course of a week in organoid culture. Modulating metabolism through UK5099 treatment inhibits the basal to luminal differentiation, as indicated by low K8 expression.

In a more detailed experiment looking at the effects of vehicle vs. UK5099-treatment in the presence of different modes of androgen blockade, Enzalutamide of chemical castration (-DHT), lineage identity was measured through luminal marker K8, basal marker K5, and basal marker p63Δn (Figure 2b, c, d). There was higher expression of K8 in vehicle treated organoids compared to UK5099 illustrating that basal-derived organoids differentiate into a more luminal phenotype. UK5099 inhibits this lineage transition. In both vehicle and UK5099-treated organoids, castration decreased K8 expression. Enzalutamide increased K8 expression in UK5099-treated organoids. This shows that lineage identity is sensitive to modulations in metabolism and AR blockade (Figure 2b, c). K5 expression was higher in UK5099-treated organoids, providing further evidence that UK5099-treated organoids retain their basal identity. p63Δn was higher in control compared to castration in both groups, and higher in UK5099-treated organoids compared to vehicle (Figure 3b). This indicates that UK5099 organoids have a greater basal phenotype and that castration decreases the basal identity.

Blocking mitochondrial pyruvate uptake affects AR expression and response to AR blockade

To further investigate the effects of UK5099 treatment on sensitivity to androgen pathway inhibitors, basal-derived organoids were treated with vehicle or UK5099, and then with control, chemical castration, or Enzalutamide, an androgen receptor pathway inhibitor. First, AR expression and target gene expression was validated. Based on RNAseq data and a literature review, several potential AR target genes to probe for were identified. The genes included were Tmprss2, HoxB13, and Nkx3.1.

AR expression is highest in both vehicle and UK5099 control groups. In vehicle treated organoids, AR expression is lower in castration than with Enzalutamide treatment. In UK5099 treated organoids, AR expression is lower with Enzalutamide than with castration (Figure 3a, b). AR remained high in the total mouse prostate, but had two bands of distinct sizes. Interestingly, UK5099 lysates that had previously shown a reduction in AR in western blots did not have a detectable decrease in this experiment, suggesting there may be an issue with the antibody used (Figure 3c). The expression of AR target Tmprss2 did not follow the same trend. While Tmprss2 bands do not show great differences visually, differences emerge when quantified. In vehicle treated organoids, control had higher Tmprss2 than castration, which was higher than Enzalutamide treatment. In UK5099-treated organoids, castration generated the highest expression. This shows that in UK5099-treated organoids, Tmprss2 expression is less sensitive to the effects of castration (Figure 3d, e). Tmprss2 did not follow the expression pattern of AR in both vehicle and UK5099-treated organoids. As for additional AR targets, HOXB13 and Pbsn were only expressed in total mouse prostate, making them unreliable markers of AR activity in organoids (Figure 3d, f).

PCNA was used as a proliferation marker and cleaved caspase 3 was used as a cell death marker. There were no large differences between samples in PCNA or cleaved caspase 3, but there appears to be slightly higher cleaved caspase 3 in both castration treatments, depicting greater cell death (Figure 3g).

An organoid growth size quantification assay was developed to understand what regulates castration resistance in 3D *ex vivo* basal-derived organoid culture. Organoid growth was measured through quantification of microscopy images. Organoid growth was initially measured after 6 days of castration treatment (Figure 4a). Results show that castration significantly decreased relative size in vehicle-treated organoids, yet appeared to increase relative size in UK5099-treated organoids (Figure 4b). Enzalutamide treatment had a similar, but less pronounced effect (Figure 4c). Differences between vehicle, castration, and Enzalutamide treatment are greater in vehicle-treated organoids. The experiment was followed with a time series that measured organoid diameter every two days post castration onset (Figure 5a). At day 0, vehicle and UK5099-treated organoids were roughly the same size with UK5099-treated organoids being slightly larger. At day 2, vehicle-treated organoids were larger than UK5099-treated organoids, with minimal differences between castrated and control. At day 4, there was the greatest difference in control and castrated organoid size, but less differences between vehicle and UK5099-treated organoids. Organoid size was difficult to determine for UK5099-treated organoids because many of them had a blebbed phenotype making it difficult to accurately determine the diameter (Figure 5c). Additionally, many smaller organoids that previously could not be seen nor measured were able to be visualized during day 4, leading to greater variability in organoid diameter. At day 6, the relative sizes of the different groups matched the previous trend seen in the initial experiment, but were less drastic. UK5099-treated organoids were larger than vehicle-treated organoids, but there were smaller differences

between control and castrated organoids. This shows that the effect of modulating metabolism on castrated organoids varies with the duration of castration. Overall, the data show that modulating metabolism and castration can alter organoid growth. AR blockade can affect organoid size and have differential effects with altered metabolism.

Blocking mitochondrial pyruvate uptake decreases TNF/NFkB signaling and increases Wnt/ β-catenin signaling

Expression of proteins associated with pathways that affect luminal differentiation in the prostate was evaluated in vehicle vs. UK5099-treated organoids. The TNF/NFkB pathway has been shown to suppress luminal differentiation while Notch, Wnt/β-catenin, EGFR, and KLF5 have been shown to promote luminal differentiation[26,27].

In vehicle vs. UK5099-treated organoids, expression of p-p65 indicating activation of the NFkB pathway decreased with UK5099-treatment along with decreased luminal expression shown by K8 (Figure 6a). In vehicle vs. UK5099-treated organoids, expression of EGFR pathway indicators p-ERK and p-AKT were relatively similar, suggesting that the pathway does not play a major role in lineage identity shifts caused by UK5099 (Figure 6b).

A subcellular fractionation was used to visualize β-catenin translocation from the membrane to the nucleus where it acts as a transcription factor when activated. In vehicle vs. UK5099-treated organoids, there was greater translocation of β-catenin to the nucleus (Figure 6c). However, with a 20 hour timepoint, there was increased nuclear soluble β-catenin with vehicle-treated organoids, showing that levels change over time (Figure 7).

Blocking mitochondrial pyruvate uptake increases nuclear translocation of citrate synthase, OGDH, and MDH2

Previous literature has shown that the translocation of citric acid cycle enzymes may be associated with epigenetic and zygotic gene expression, providing potential insight on UK5099 action[28]. The subcellular location of several citric acid cycle enzymes was observed with vehicle vs. UK5099-treatment (Figure 8a). UK5099-treatment lead to increased nuclear translocation of citrate synthase, OGDH, MDH2 (Figure 8b). PDHA, an enzyme normally found in the mitochondrial membrane also translocated to the nucleus with both vehicle and UK5099 treatment (Figure 8b).

5. DISCUSSION

This project sought to understand the effect of modulating metabolism on lineage identity and AR blockade in basal-derived organoids. Clinically, therapy resistance is often accompanied by a loss of luminal identity and a gain of basal and neuroendocrine features[16,29]. It is essential to understand this transition to learn how to drive luminal differentiation, increase sensitivity to therapy, and decrease resistance.

Since UK5099 has been shown to inhibit luminal differentiation in basal-derived organoids, I originally hypothesized that they would be less sensitive to AR blockade given their basal characteristics. Several experimental findings support this hypothesis. K8, K5, and p63Δn expression shows that vehicle-treated basal-derived organoids are able to differentiate into luminal cells, but UK5099 blocks this transition and retains the basal phenotype. These findings are similar to what has been seen in the study by Mahendralingam et al. where glycolysis was enriched in basal cells and oxidative phosphorylation was enriched in luminal cells in mammary epithelial cells in the context of breast cancer[22]. Altered lineage identity may be related to the effects of castration on AR expression. AR expression in castrated organoids decreased far more in vehicle-

treated organoids than UK5099-treated organoids, showing that AR expression in UK5099-treated castrated organoids is less dependent on external androgens. This is further supported by AR target gene Tmprss2 expression, which increased in UK5099-treated castrated organoids, but decreased in vehicle-treated castrated organoids. The organoid size quantification assay developed to understand what regulates castration experiments was helpful in determining the role of AR blockade and altered metabolism. The assay suggests that UK5099-treated organoids are less sensitive to AR blockade. This can be seen where vehicle-treated organoids significantly decrease in size in castrated conditions, while UK5099-treated organoids actually appear to increase in size. However, these results are inconsistent over time potentially indicating that the time after castration can affect relative differences in organoid size. While there are no large differences in AR expression in control vehicle and UK509-treated organoids, the results are most distinct with AR blockade through castration or Enzalutamide. Collectively, the results show that altered metabolism can affect response to AR blockade.

These findings are in line with the clinical research study published by Tewari et al. Tewari et al. performed RNAseq on patients who were exceptional responders and non-responders to androgen pathway inhibitor treatment[30]. Analysis by the Goldstein Laboratory showed that patients who were exceptional responders had a higher luminal signature and a lower basal signature than non-responders. Exceptional responders also had higher MPC1 and 2 expression than non-responders. These results in human prostate cancer correlate to our findings in mouse-derived nonmalignant basal organoids that MPC inhibition and a basal-phenotype decrease sensitivity to AR blockade.

Altered expression of the TNF/NFkB pathway and the Wnt/β-catenin signaling pathway suggests potential involvement in lineage identity shifts associated with UK5099-treatment. The

Wnt/β-catenin pathway initially had higher expression in vehicle organoids at the 20 hour timepoint, but then had the opposite trend in the longer timepoint. It is possible that the pathways changed expression according to the literature soon after UK5099 treatment, but the timepoint observed allowed organoids to overcompensate for the change and pathways rebounded past normal expression levels.

Previous literature by Nagaraj et al., has shown that transient translocation of citric acid cycle enzymes plays a prominent role in zygotic gene activation and epigenetic remodeling[28]. For example, alpha-ketoglutarate in the nucleus is important for demethylation of DNA and histones, and acetyl-CoA, a common product from metabolic reactions, promotes histone acetylation[28]. Increased translocation of OGDH, MDH2, and citrate synthase with UK5099-treatment suggests that UK5099 may induce epigenetic changes that alter gene expression. Interestingly, the extra-mitochondrial localization of PDHA as observed with both vehicle and UK5099-treatment is a phenotype found in cancer cell lines and shown to be important for the activation of zygotic genes, showing a potential connection between metabolic enzymes and differentiation[28]. Research by Berger, et al., has also observed epigenetically-driven changes in lineage plasticity medicated by N-Myc in advanced prostate cancer[31]. The current results in combination with previous literature support a potential epigenetic mechanism behind lineage identity changes[10,11,28,31].

The strength of this study was its use of multiple techniques to answer experimental questions leading to increased validity of findings. For instance, the use of a western blot and organoid size assay to provided two different methods of observing organoid growth. What could be improved is the reliability of the organoid size assay, as it seems that the number of days post-castration can influence the relative trend in organoid growth. Future directions should consider alternative experiments to validate findings such as investigating RNA expression and ensuring

that it aligns with protein expression or using a cell cycle flow cytometry assay to measure cell growth and proliferation. Future experiments could also take different approaches to modulating metabolism such as upregulating oxidative phosphorylation, investigate epigenetic changes with UK5099-treatment, and altering the expression of genes of interest through viral overexpression or siRNA knockdown. All of these methods would increase the accuracy of the results by investigating at multiple cellular levels. Most importantly, future experiments should seek to understand the mechanism behind the effects of lineage identity in response to AR blockade to identify therapeutic strategies to sensitize tumors to therapy.

6. FIGURES

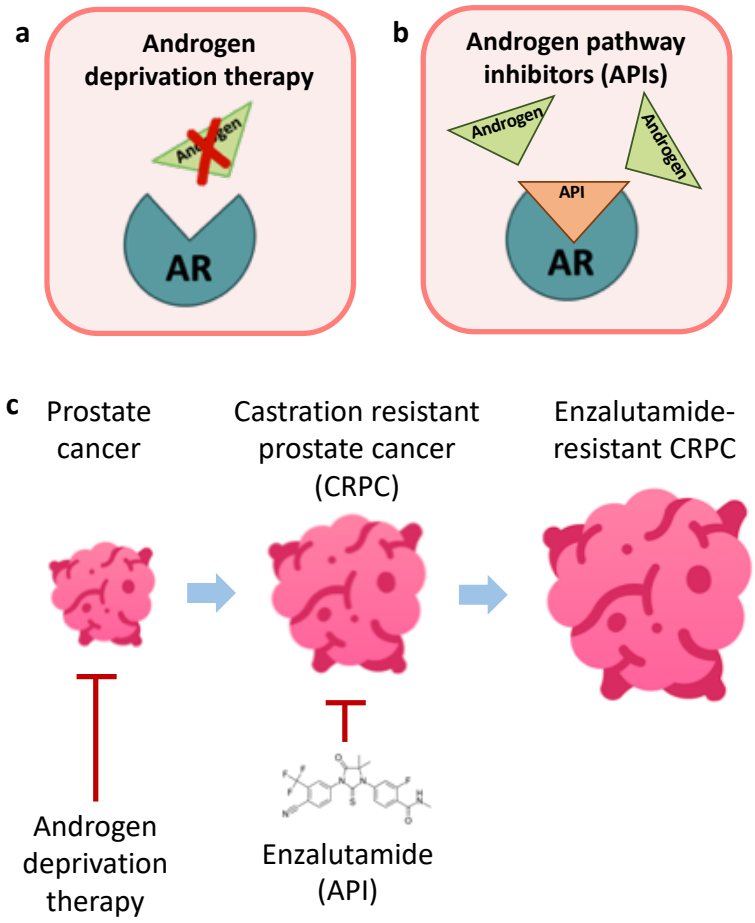

Figure 1. Schematic of prostate cancer progression and treatments. (a) Mechanism of androgen deprivation therapy. **(b)** Mechanism of androgen pathway inhibitors (APIs). **(c)** Progression of prostate cancer and available treatments.

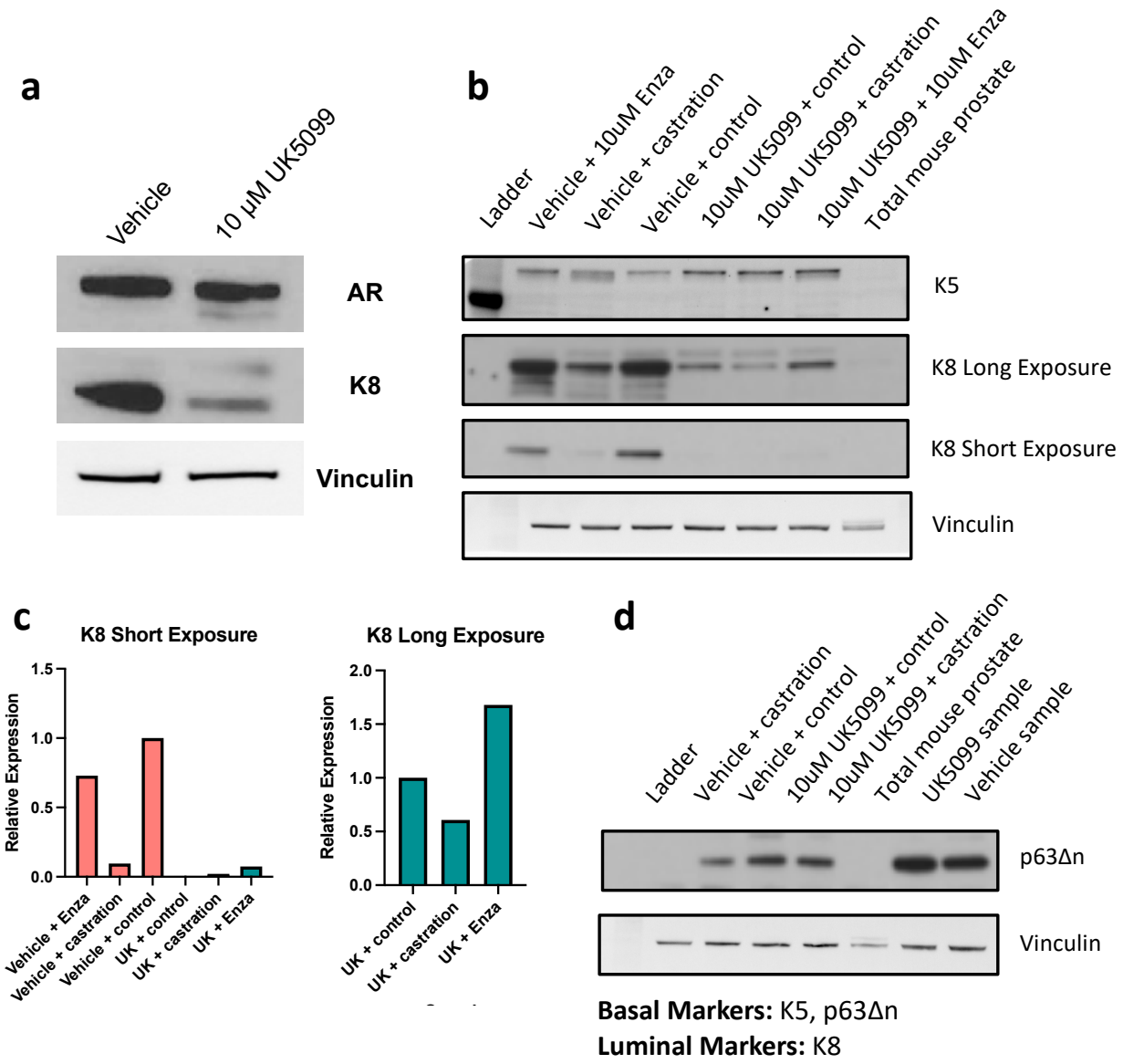

Figure 2. Protein expression of lineage identity markers. Basal markers probed for were K5 and p63Δn. Luminal marker probed for was K8. **(a)** Western blot of AR, K8, and vinculin (loading control) in vehicle vs. 10μM UK5099-treated organoids. **(b)** Western blot of K5 and K8 with vehicle vs. 10μM UK5099 pre-treatment followed by control, 10μM Enzalutamide (Enza), or chemical castration (-DHT). **(c)** Relative quantification of K8 from (b). **(d)** Western blot of p63Δn with vehicle vs. 10μM UK5099 pre-treatment followed by control or chemical castration (-DHT).

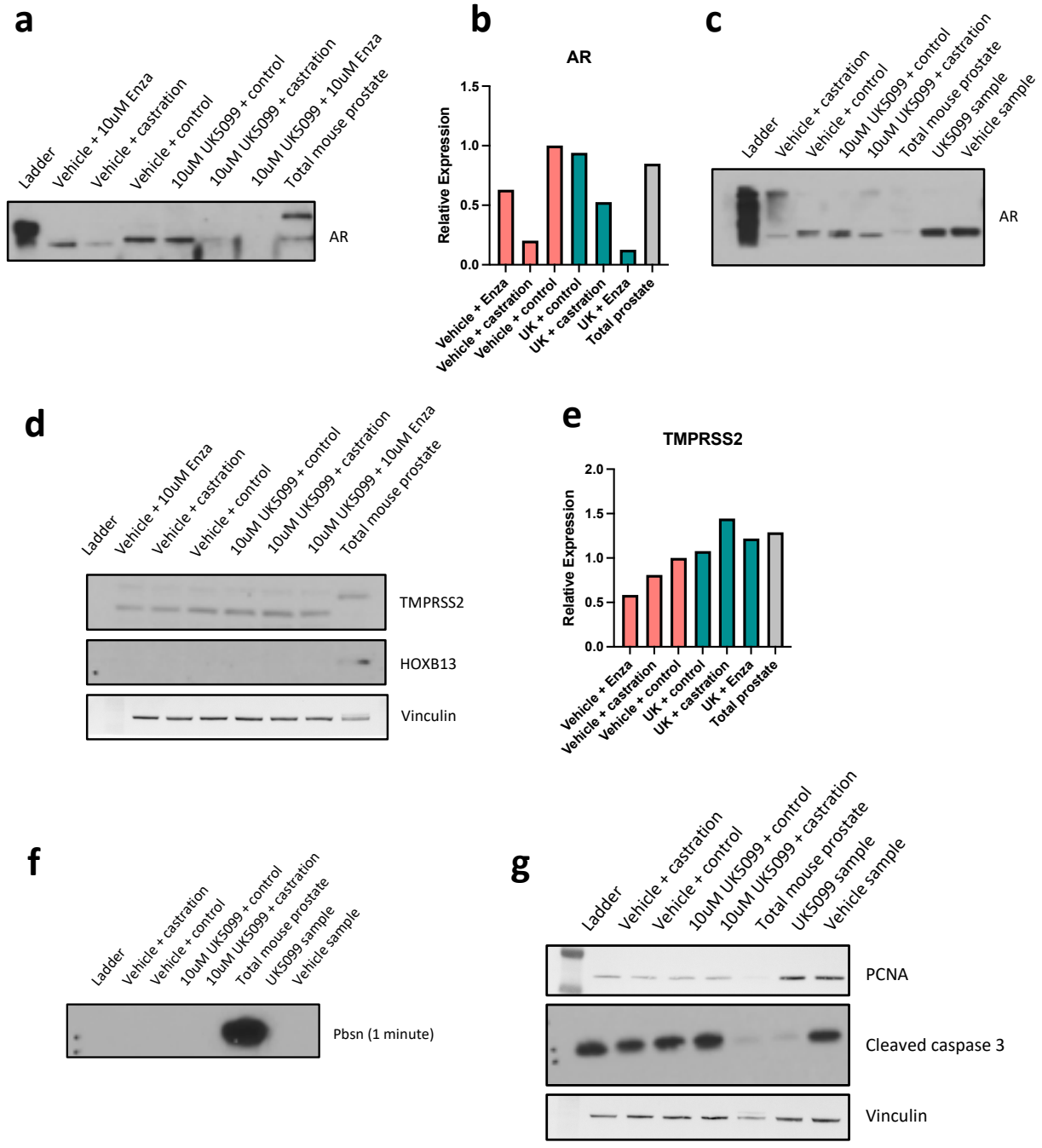

Figure 3. Protein expression of AR and AR target genes in basal-derived organoids treated with 10μM UK5099 and androgen blockade. (a) Western blot band for AR with vehicle vs. 10μM UK5099 pre-treatment followed by control, 10μM Enzalutamide (Enza), or chemical castration (-DHT) or total mouse prostate. **(b)** Relative quantification of AR from (a). **(c)** Western

blot band for AR with vehicle vs. 10μM UK5099 pre-treatment followed by control or chemical castration (-DHT) or total mouse prostate. 'UK5099 sample' and 'vehicle sample' lanes on the right represent previously collected lysate from vehicle vs. 10μM UK5099 treated organoids. **(d)** Western blot bands of AR target genes TMPRSS2 and HOXB13 with vehicle vs. 10μM UK5099 pre-treatment followed by control, 10μM Enzalutamide (Enza), or chemical castration (-DHT) or total mouse prostate. **(e)** Relative quantification of TMPRSS2 from (d). **(f)** Western blot band of AR target gene Pbsn vehicle vs. 10μM UK5099 pre-treatment followed by control or chemical castration (-DHT) or total mouse prostate. 'UK5099 sample' and 'vehicle sample' lanes on the right represent previously collected lysate from vehicle vs. 10μM UK5099 treated organoids. **(g)** Western blot bands for PCNA (proliferation marker) or cleaved caspase 3 (death marker) with with vehicle vs. 10μM UK5099 pre-treatment followed by control or chemical castration (-DHT) or total mouse prostate. 'UK5099 sample' and 'vehicle sample' lanes on the right represent previously collected lysate from vehicle vs. 10μM UK5099 treated organoids.

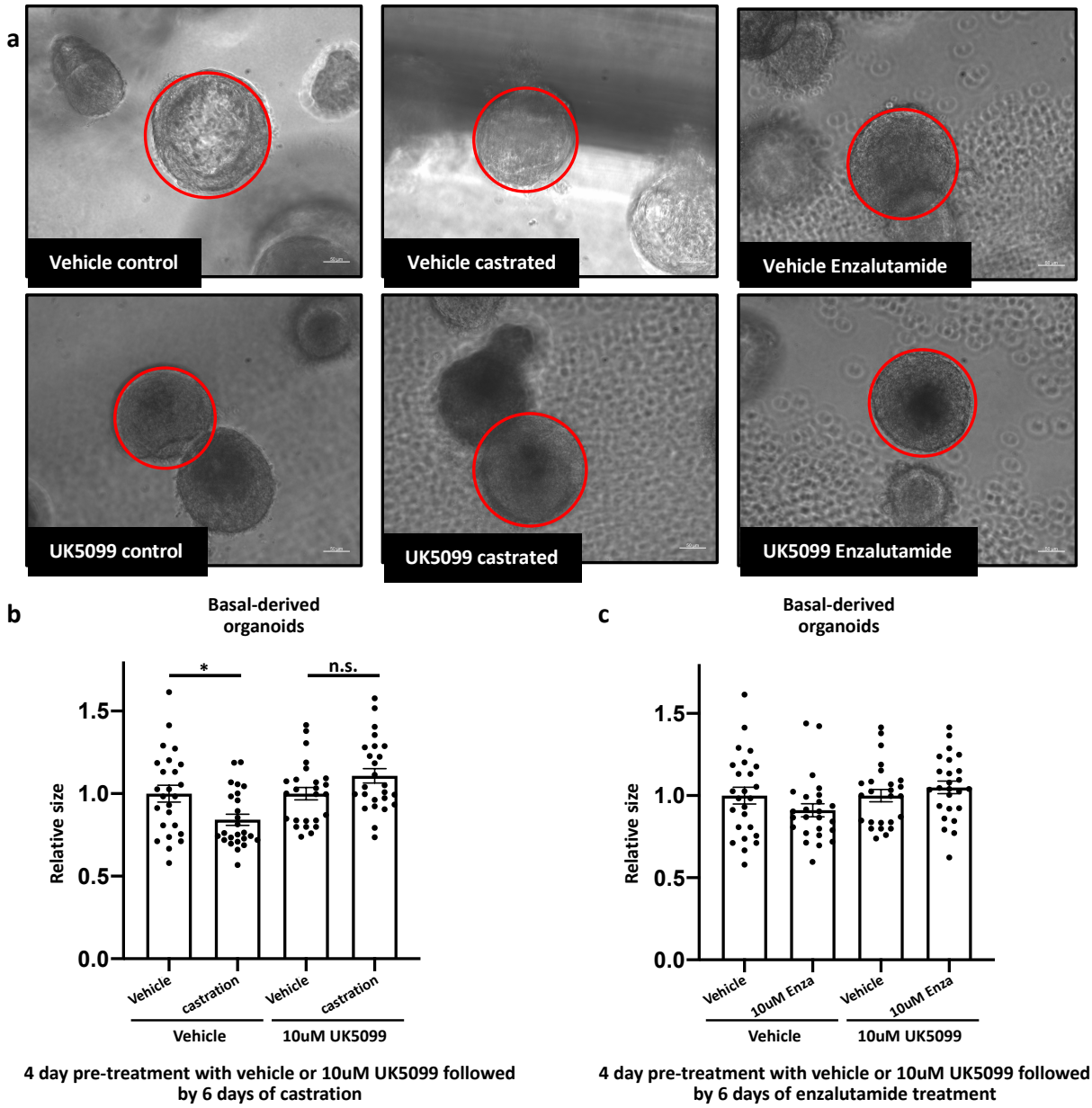

Figure 4. Average organoid diameter of basal-derived organoids treated with UK5099 (4 day pre-treatment) and androgen blockade (6 days). (a) Representative images of organoids from each sample. **(b)** Quantification of vehicle and 10 µM UK5099 treated organoids with castration. **(c)** Quantification of vehicle and 10 µM UK5099 treated organoids with 10 µM Enzalutamide (Enza).

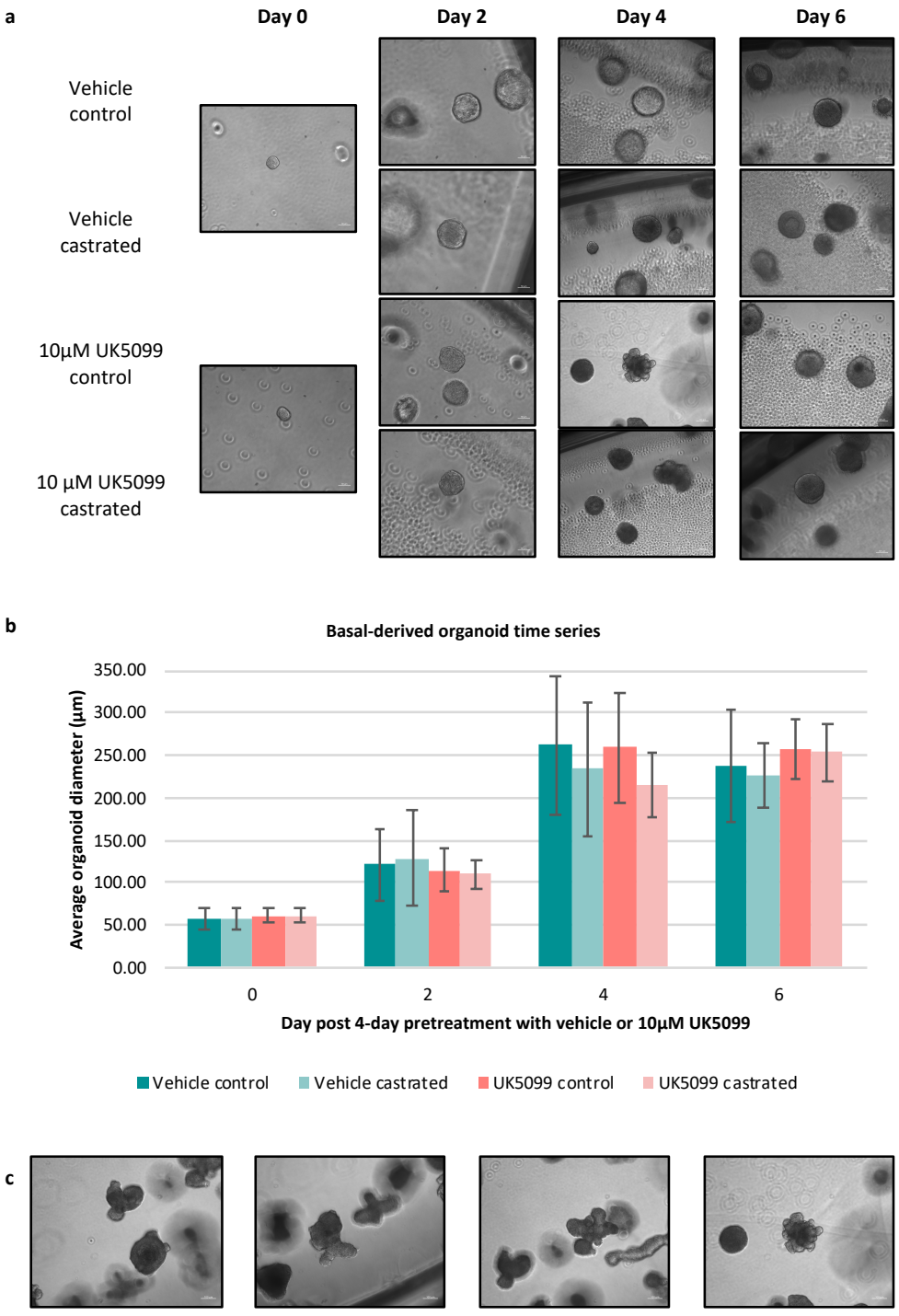

Figure 5. Time series of average organoid diameter of basal-derived organoids treated with UK5099 (4 day pre-treatment) and castration (6 days). (a) Representative images of organoids

from each sample. **(b)** Quantification of vehicle and 10 µM UK5099 treated organoids with castration. **(c)** Day 4 UK5099-treated organoid blebbed phenotype.

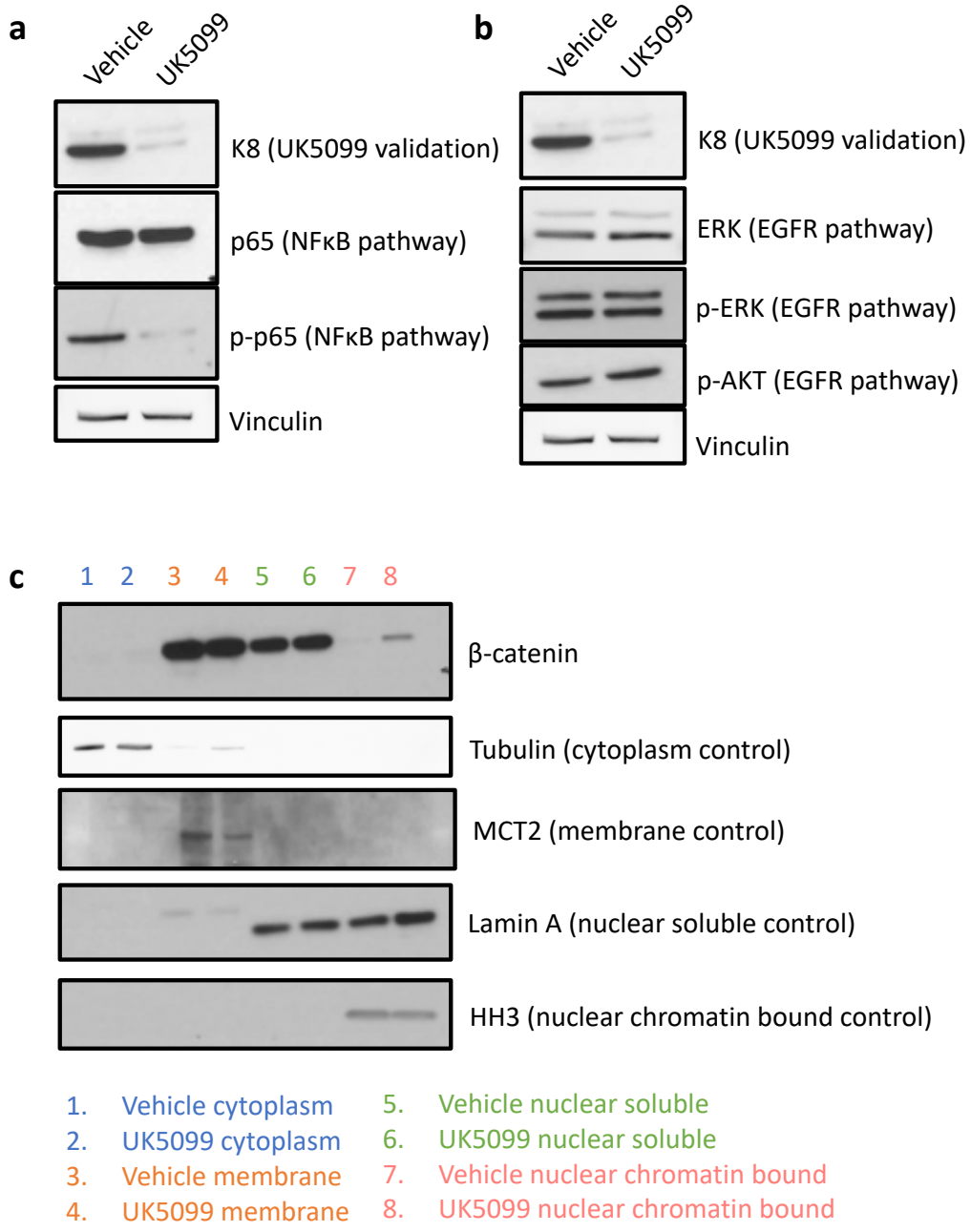

Figure 6. Protein expression of pathways that regulate differentiation in the prostate after 7 days of treatment. (a) NFkB pathway in vehicle vs. UK5099-treated organoids. **(b)** EGFR

pathway vehicle vs. UK5099-treated organoids. **(c)** Subcellular fractionation of Wnt/β-catenin pathway vehicle vs. UK5099-treated organoids.

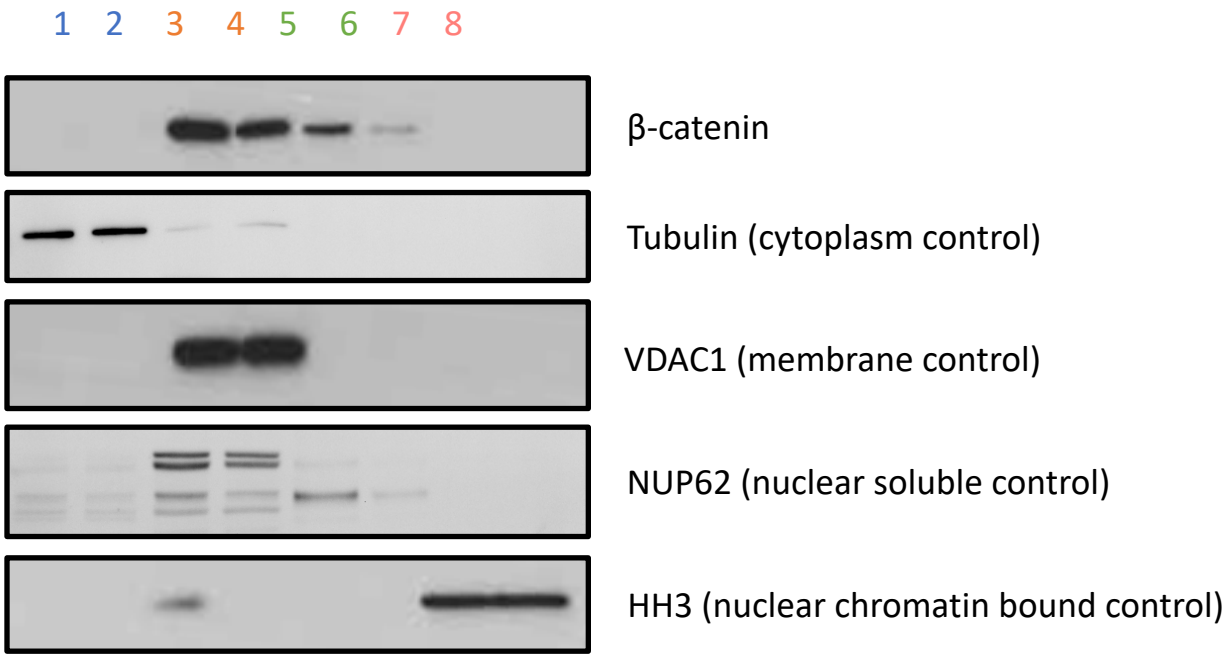

Samples

1. Vehicle cytoplasm
2. UK5099 cytoplasm
3. Vehicle membrane
4. UK5099 membrane
5. Vehicle nuclear soluble
6. UK5099 nuclear soluble
7. Vehicle nuclear chromatin bound
8. UK5099 nuclear chromatin bound

Figure 7. Protein expression of pathways that regulate differentiation in the prostate after 4 days culture and 20 hours treatment. (a) Subcellular fractionation of Wnt/β-catenin pathway vehicle vs. UK5099-treated organoids.

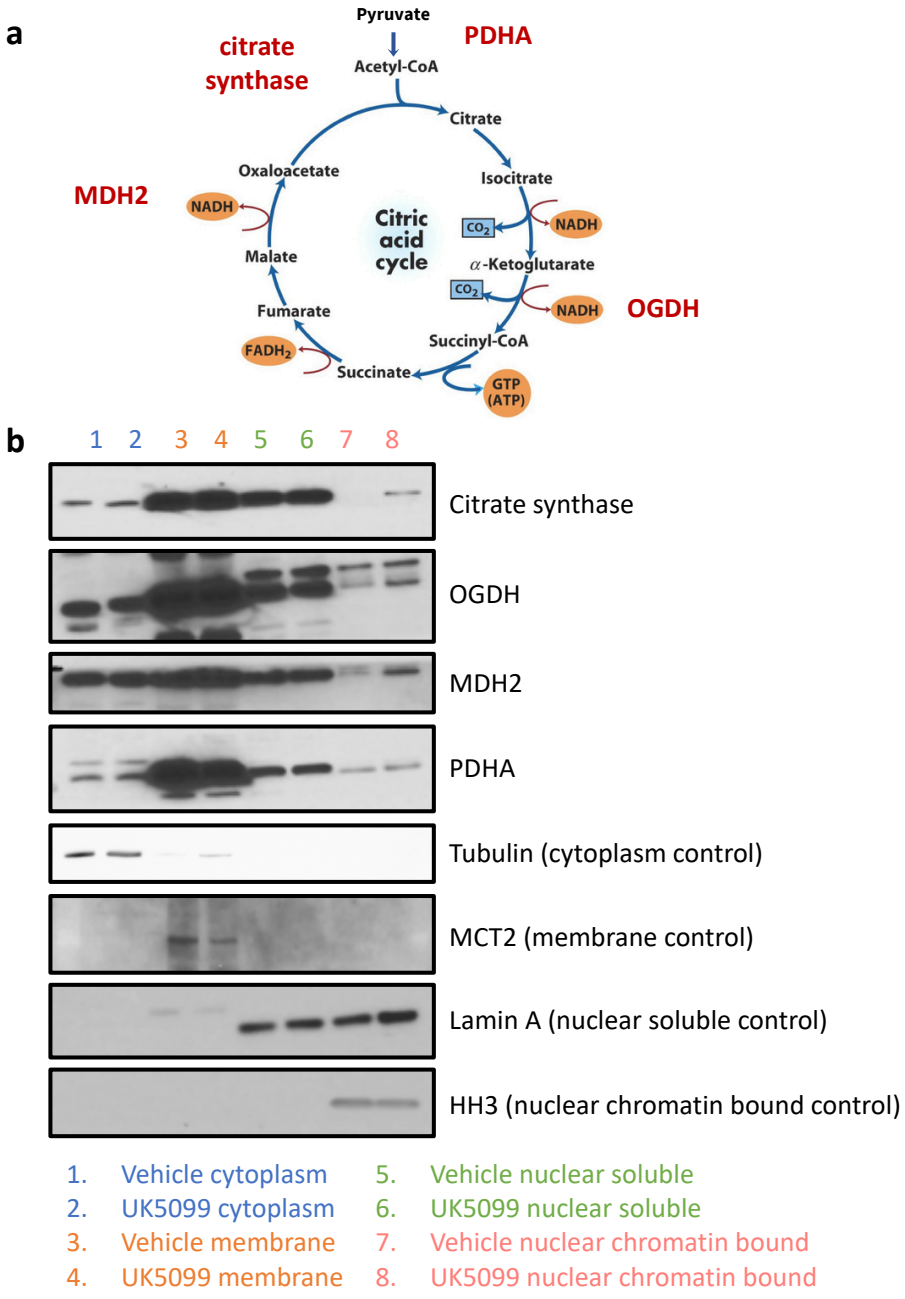

Figure 8. Protein expression and localization of citric acid cycle enzymes. (a) Location of selected enzymes in citric acid cycle. **(b)** Localization and expression of citrate synthase, OGDH, MDH2, and PDHA in vehicle vs. UK5099-treated organoids.

7. REFERENCES

1. American Cancer Society. Key Statistics for Prostate Cancer | Prostate Cancer Facts. https://www.cancer.org/cancer/prostate-cancer/about/key-statistics.html (2022). Accessed March 30, 2022.
2. Fujita, K. & Nonomura, N. Role of Androgen Receptor in Prostate Cancer: A Review. *World J Mens Health* **37**, 288–295 (2019).
3. Tan, M. E., Li, J., Xu, H. E., Melcher, K. & Yong, E. Androgen receptor: structure, role in prostate cancer and drug discovery. *Acta Pharmacol Sin* **36**, 3–23 (2015).
4. Hoffman, R. M. Clinical practice. Screening for prostate cancer. *N Engl J Med* **365**, 2013–2019 (2011).
5. Castoria, G. *et al.* Androgen-induced cell migration: role of androgen receptor/filamin A association. *PLoS One* **6**, e17218 (2011).
6. Heinlein, C. A. & Chang, C. Androgen receptor in prostate cancer. *Endocr Rev* **25**, 276–308 (2004).
7. Che, M. *et al.* Opposing transcriptional programs of KLF5 and AR emerge during therapy for advanced prostate cancer. *Nat Commun* **12**, 6377 (2021).
8. Chandrasekar, T., Yang, J. C., Gao, A. C. & Evans, C. P. Mechanisms of resistance in castration-resistant prostate cancer (CRPC). *Transl Androl Urol* **4**, 365–380 (2015).
9. Chang, K.-H., Ercole, C. E. & Sharifi, N. Androgen metabolism in prostate cancer: from molecular mechanisms to clinical consequences. *Br J Cancer* **111**, 1249–1254 (2014).
10. Ge, R. *et al.* Epigenetic modulations and lineage plasticity in advanced prostate cancer. *Annals of Oncology* **31**, 470–479 (2020).

11. Davies, A., Zoubeidi, A. & Selth, L. A. The epigenetic and transcriptional landscape of neuroendocrine prostate cancer. *Endocr Relat Cancer* **27**, R35–R50 (2020).
12. Bishr, M. & Saad, F. Overview of the latest treatments for castration-resistant prostate cancer. *Nat Rev Urol* **10**, 522–528 (2013).
13. Scher, H. I. *et al.* Increased survival with enzalutamide in prostate cancer after chemotherapy. *N Engl J Med* **367**, 1187–1197 (2012).
14. Alumkal, J. J. *et al.* Transcriptional profiling identifies an androgen receptor activity-low, stemness program associated with enzalutamide resistance. *PNAS* **117**, 12315–12323 (2020).
15. Beltran, H. *et al.* The Role of Lineage Plasticity in Prostate Cancer Therapy Resistance. *Clin Cancer Res* **25**, 6916–6924 (2019).
16. Tiwari, R. *et al.* Androgen deprivation upregulates SPINK1 expression and potentiates cellular plasticity in prostate cancer. *Nature Communications* **11**, 384 (2020).
17. Park, J. W. *et al.* Prostate epithelial cell of origin determines cancer differentiation state in an organoid transformation assay. *Proc Natl Acad Sci U S A* **113**, 4482–4487 (2016).
18. Kurita, T., Medina, R. T., Mills, A. A. & Cunha, G. R. Role of p63 and basal cells in the prostate. *Development* **131**, 4955–4964 (2004).
19. Xie, Q. *et al.* Dissecting cell-type-specific roles of androgen receptor in prostate homeostasis and regeneration through lineage tracing. *Nat Commun* **8**, 14284 (2017).
20. Rodríguez-Colman, M. J. *et al.* Interplay between metabolic identities in the intestinal crypt supports stem cell function. *Nature* **543**, 424–427 (2017).
21. Yu, Y. *et al.* Glutamine metabolism regulates proliferation and lineage allocation in skeletal stem cells. *Cell Metab* **29**, 966-978.e4 (2019).

22. Mahendralingam, M. J. *et al.* Mammary epithelial cells have lineage-rooted metabolic identities. *Nat Metab* **3**, 665–681 (2021).
23. Baksh, S. C. *et al.* Extracellular serine controls epidermal stem cell fate and tumour initiation. *Nature Cell Biology* **22**, 779–790 (2020).
24. Schell, J. C. *et al.* Control of intestinal stem cell function and proliferation by mitochondrial pyruvate metabolism. *Nature Cell Biology* **19**, 1027–1036 (2017).
25. Drost, J. *et al.* Organoid culture systems for prostate epithelial and cancer tissue. *Nat Protoc* **11**, 347–358 (2016).
26. Zhang, B. *et al.* Klf5 acetylation regulates luminal differentiation of basal progenitors in prostate development and regeneration. *Nat Commun* **11**, 997 (2020).
27. Centonze, A. *et al.* Heterotypic cell–cell communication regulates glandular stem cell multipotency. *Nature* **584**, 608–613 (2020).
28. Nagaraj, R. *et al.* Nuclear Localization of Mitochondrial TCA Cycle Enzymes as a Critical Step in Mammalian Zygotic Genome Activation. *Cell* **168**, 210-223.e11 (2017).
29. Tuerff, D., Sissung, T. & Figg, W. D. Cellular identity crisis: Antiandrogen resistance by lineage plasticity. *Cancer Biol Ther* **18**, 841–842 (2017).
30. Tewari, A. K. *et al.* Molecular features of exceptional response to neoadjuvant anti-androgen therapy in high-risk localized prostate cancer. *Cell Reports* **36**, 109665 (2021).
31. Berger, A. *et al.* N-Myc–mediated epigenetic reprogramming drives lineage plasticity in advanced prostate cancer. *J Clin Invest* **129**, 3924–3940 (2019).